Metal Matrix Composites

Focus on Alloys and Lattice Dynamics

Materials Science and Technologies

Suzanne N. Fitzgerald
Editor

NOVA

MATERIALS SCIENCE AND TECHNOLOGIES

METAL MATRIX COMPOSITES

FOCUS ON ALLOYS AND LATTICE DYNAMICS

SUZANNE N. FITZGERALD
EDITOR

Nova Science Publishers, Inc.
New York

For permission to use material from this book please contact us:
Telephone 631-231-7269; Fax 631-231-8175
Web Site: http://www.novapublishers.com

Library of Congress Cataloging-in-Publication Data

Metal matrix composites : focus on alloys and lattice dynamics / editor, Suzanne N. Fitzgerald.
p. cm.
Includes bibliographical references and index.
ISBN 978-1-61324-483-8 (hardcover : alk. paper) 1. Metallic composites. I. Fitzgerald, Suzanne N.
TA481.M4465 2011
620.1'6--dc23

2011012844

Published by Nova Science Publishers, Inc. †New York

MATERIALS SCIENCE AND TECHNOLOGIES

METAL MATRIX COMPOSITES

FOCUS ON ALLOYS AND LATTICE DYNAMICS

MATERIALS SCIENCE AND TECHNOLOGIES

Additional books in this series can be found on Nova's website under the Series tab.

Additional E-books in this series can be found on Nova's website under the E-book tab.

PREFACE

This book presents current research in the study of metal matrix composites, with a particular focus on alloys and lattice dynamics. Topics discussed include lattice dynamics of equiatomic alkali binary alloys and liquid alloys; lattice dynamics of liquid alloys, liquid metals and solid metallic elements; generation and validation of failure assessment diagrams for high strength alloys utilizing the inherent flaw model and the effect of applied load on the characteristics of reversible martensitic transformation during thermal cycling treatment of a monocrystalline Cu-13.5Al-4Ni alloy.

Chapter 1 - Modifications are made in the inherent flaw model of Waddoups, Eisenman and Kaminski (known as the WEK model) to improve fracture strength evaluation of cracked bodies. A relation is proposed for the generation of failure assessment diagram and validated by comparing with the test data of different high strength alloys.

Chapter 2 - The changes in the characteristics of the reversible martensitic transformation (RMT), caused by different applied loads during thermal cycling treatments under load (TCL) were investigated in a monocrystalline Cu-13.5wt.%Al-4.0wt.%Ni alloy. The TCL was performed by an accumulation of 300 cycles in the temperature interval between 0 °C (shortly below the M_f) and 90 °C (just above A_f). These treatments were conducted both load-free and under three different applied load of 0.1, 0.2 and 0.5 kg, corresponding to 0.056, 0.112 and 0.280 MPa, respectively. After each distinct treatment condition, the alloy specimen was characterized by X-ray diffraction, optical microscopy, differential calorimetry and microhardness. It was found that the TCL promotes significant changes that are related to the resulting structures and characteristics of the RMT. An increase in the applied load causes a sensible decrease in the critical temperature interval associated with the RMT. Moreover, a decrease in both, the thermal hysteresis and the enthalpy, as well as an increase in the microhardness were also observed with applied load. This behavior is not only a consequence of a decrease in the martensitic variants but also related to the greater stability of an intermediate state, which facilitates the transformation mechanism.

Chapter 3 - The computations of the lattice dynamics of equiatomic alkali binary alloys to second order in local model potential is discussed in terms of real-space sum of Born von Karman central force constants. The local field correlation functions due to Hartree (H) and Ichimaru-Utsumi (IU) are used to investigate influence of the screening effects on the aforesaid properties. Results for the lattice constants i.e. C_{11}, C_{12}, C_{44}, $C_{12} - C_{44}$, C_{12}/C_{44} and bulk modulus B obtained using the H-local field correction function have higher values in comparison with the results obtained for the same properties using IU local field correction function. The results for the Shear modulus (C'), deviation from Cauchy's relation, Poisson's ratio σ , Young modulus Y , propagation velocity of elastic waves, phonon dispersion curves and degree of anisotropy A are highly appreciable for equiatomic alkali binary alloys.

Chapter 4 - In the present chapter, the lattice dynamical properties of some equiatomic liquid alkali binary alloys are reported in second order approach through the equation given by Hubbard and Beeby (HB). The pair correlation function $g(r)$ is directly computed from the interatomic pair potential, which is used in the present computation. Two different forms of local field correction functions proposed by Hartree (H) and Ichimaru-Utsumi (IU) are used in the present study the screening dependence of the phonon frequencies in the equiatomic liquid alkali binary alloys. Thermodynamic and elastic properties of equiatomic liquid alkali binary alloys are reported from the long wave length limits of the phonon dispersion curves (PDC). The pseudo-alloy-atom (PAA) model is applied for the first time for the alloying elements.

Chapter 5 - In the present chapter, the lattice dynamical properties of some alkali metals are reported in second order approach through the equation given by Hubbard and Beeby (HB). The pair correlation function $g(r)$ is directly computed from the interatomic pair potential, which is used in the present computation. Two different forms of local field correction functions proposed by Hartree (H) and Ichimaru-Utsumi (IU) are used in the present study the screening dependence of the phonon frequencies in the metallic elements.

Thermodynamic and elastic properties of alkali metals are reported from the long wave length limits of the phonon dispersion curves (PDC).

Chapter 6 - The computations of the lattice dynamics of solid metallic elements to second order in local model potential is discussed in terms of real-space sum of Born von Karman central force constants. The local field correlation functions due to Hartree (H) and Ichimaru-Utsumi (IU) are used to investigate influence of the screening effects on the aforesaid properties. Results for the lattice constants i.e. C_{11}, C_{12}, C_{44}, $C_{12}-C_{44}$, C_{12}/C_{44} and bulk modulus B obtained using the H-local field correction function have higher values in comparison with the results obtained for the same properties using IU local field correction function. The results for the Shear modulus (C'), deviation from Cauchy's relation, Poisson's ratio σ, Young modulus Y, propagation velocity of elastic waves, phonon dispersion curves and degree of anisotropy A are highly appreciable for metallic elements.

CONTENTS

In: Metal Matrix Composites
Editor: Suzanne N. Fitzgerald
ISBN: 978-1-61324-483-8

Chapter 1

GENERATION AND VALIDATION OF FAILURE ASSESSMENT DIAGRAMS FOR HIGH STRENGTH ALLOYS UTILIZING THE INHERENT FLAW MODEL

S. Rajakumar and T. Christopher*
Faculty of Mechanical Engineering, Government College of Engineering,
Perumalpuram, Tirunelveli-627 007, India

ABSTRACT

Modifications are made in the inherent flaw model of Waddoups, Eisenman and Kaminski (known as the WEK model) to improve fracture strength evaluation of cracked bodies. A relation is proposed for the generation of failure assessment diagram and validated by comparing with the test data of different high strength alloys.

Keywords: High strength alloys, center crack tensile specimen, inherent flaw model, failure assessment diagram, fracture strength

* Corresponding author: E-mail: christo59@rediffmail.com

NOMENCLATURE

a_{ci}	Damage zone size
c	Half crack length
K_F, *m, p*	Fracture parameters in equation (1)
K_{IFM}, δ_{aci}	Fracture parameters in equation (8)
$K_Q\left(\equiv \sigma_{NC}^{\infty}\sqrt{\pi c}\right)$	Parameter in Failure assessment diagram
t	Specimen thickness
W	Specimen width
Y	Finite width correction factor
σ	Applied far field stress
σ_{NC}^{∞}	Fracture strength of a wide specimen
σ_{NC}	Fracture strength of finite width specimen
σ_o	Ultimate tensile strength (unnotched strength)

1. INTRODUCTION

Aerospace industry recognized two types of failure criteria: yielding and fracture. Failure due to yielding is applied to a criterion in which some functional of the stress or strain is exceeded and fracture is applied to a criterion in which an already existing crack extends according to an energy balance hypothesis. Experimentation with a variety of materials would show that the theory works well for certain materials but not for others. The safety assessment of structures without a fracture mechanics analysis is insufficient and may cause an unexpected reduction in the load carrying capacity of an actual structure due to the presence of unavoidable crack-like defects not being taken into consideration. The extraordinary success of fracture mechanics lies in its ability to combine a theoretical framework with experimentally measured critical quantities.

Several fracture analysis methods [1] were described to predict the fracture behavior of flawed structural components. None of these methods correlated well with the test data of all structural materials. Gordon [2] has reviewed several fracture-mechanics-based fitness-for-service concepts. In the failure assessment diagram or the R6 method [3], the integrity of the structure is assessed and represented in a two-dimensional way: a function of the failure strength pursuant to linear elastic fracture mechanics (LEFM) is plotted as ordinate and that pursuant to plastic collapse as abscissa. The Dugdale model [4] established the stress limits for any transitional stages between linear elastic failure and plastic collapse. Experiments largely proved these limits to be conservative. The two-parameter fracture criterion of Newman [1, 5] too, applies relations derived within the scope of LEFM. In this criterion, the two fracture parameters take account of the deviation of the stress-to-failure from the stress calculated pursuant to LEFM principles. These parameters have to be determined earlier in pretests, so-called base-line tests, conducted under identical conditions of the material. Keller, Junker and Merker [6] have carried out fracture analysis of surface cracks in cylindrical vessels applying the two-parameter fracture criterion. It was neither possible to determine satisfactorily the failure stresses of vessels by means of fracture parameters obtained from fracture mechanics specimens, nor to predict the loads to failure of the specimens by means of the vessels' fracture parameters. Zerbst *et al.* [7] have applied the recently developed European flaw assessment procedure SINTAP (Structural Integrity Assessment Procedures for European Industry) to the published fracture data [8] on steel pipes having through-wall and surface cracks subjected to internal pressure. The SINTAP procedure offers a CDF (Crack Driving Force) and a FAD (Failure Assessment Diagram) route. Both are complementary and give identical results. In the CDF route the determination of the crack tip loading in the component and its comparison with the fracture resistance of the material are two separate steps. In contrast to this philosophy, in the FAD route, a failure line is constructed by normalizing the crack tip loading with the material's fracture resistance. The assessment of the component is then based on the relative location of an assessment point with respect to this failure line.

For cracked configurations, a relation between the stress intensity factor (K_{max}) and the corresponding stress (σ_f) at failure is suggested as [9-12]:

$$K_{max} = K_F \left\{ 1 - m\left(\frac{\sigma_f}{\sigma_u}\right) - (1-m)\left(\frac{\sigma_f}{\sigma_u}\right)^p \right\} \tag{1}$$

where, σ_f is the failure stress normal to the direction of the crack in a body and σ_u is the nominal stress required to produce a plastic hinge on the net section. For the pressurized cylinders, σ_f is the hoop stress at the failure pressure of the flawed cylinder, and σ_u is the hoop stress at the failure pressure of an unflawed cylinder. For the determination of three fracture parameters (K_F, m and p), test results of simple laboratory specimens like compact tension specimens, center crack specimens etc. can be utilized. For fracture strength evaluation of any other structural configuration, the stress intensity factor corresponding to that geometry is to be used in equation (1) to develop the necessary fracture strength equation. If the values of applied stress and corresponding stress intensity factor for the specified crack size in a structure lie below the K_{max} - σ_f curve of the failure assessment diagram, the structure for that loading condition is safe.

Fracture data [13] have been compiled for selected high strength alloys (viz., steels, aluminium and titanium alloys) useful for aircraft applications. This article utilizes an improved inherent flaw model for tensile fracture strength evaluation of high strength alloys.

2. Modified Inherent Flaw Model

The stress intensity factor for a wide tensile specimen having a centre crack is expressed as

$$K_I = \sigma\sqrt{\pi c} \tag{2}$$

where σ is the applied stress and c is half crack length. Similar to Irwin's plastic zone correction, the assumption of the existence of an intense energy region of length a_{ci} (Figure1) results in the following equation for a wide centre crack tensile specimen at failure:

$$K_{Q\infty} = \sigma_{NC}^{\infty}\sqrt{\pi(c+a_{ci})} \tag{3a}$$

Here σ_{NC}^{∞} is the fracture strength of the wide tensile specimen having a centre crack of length 2c; a_{ci} is the crack- tip damage size at failure. In other words $(c + a_{ci})$ is an effective half crack length. For the case of unflawed specimens, the fracture strength equals the ultimate tensile strength (σ_o) and equation (3a) becomes

$$K_{Q\infty} = \sigma_0 \sqrt{\pi a_{ci}} \tag{3b}$$

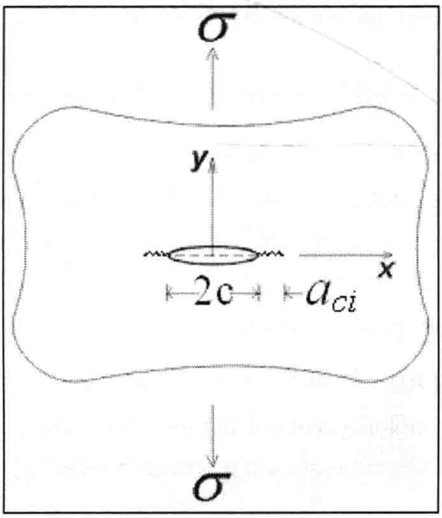

Figure 1. The characteristic length *(a_{ci})* in a center-crack wide tensile panel.

Thus, a_{ci} can be considered equivalent to the half crack length of an inherent flaw in the unflawed tensile specimen. Accordingly, this model is known as "the inherent flaw model (IFM)"or "the WEK model"[14].

From equations (3a) and (3b), one can express

$$\sigma_{NC}^{\infty} = \frac{\sigma_0}{\sqrt{\dfrac{c}{a_{ci}} + 1}} \tag{4}$$

The unknown characteristic length (a_{ci}) is to be obtained from the test data of a finite width tensile cracked specimen. The fracture Strength (σ_{NC}^{∞}) of the center crack wide tensile specimen is obtained from that of a finite width specimen (σ_{NC}) as

$$\sigma_{NC}^{\infty} = \sigma_{NC}\, Y \tag{5}$$

where the finite width correction factor [15] is,

$$Y = \sqrt{\sec\left(\frac{\pi c}{W}\right)} \tag{6}$$

where 'c' is half the crack length and W is the specimen width.

Using σ_{NC}^{∞}, σ_0 and c, the unknown characteristic (a_{ci}) is found from equation (4) as

$$a_{ci} = \frac{c}{\left(\dfrac{\sigma_0}{\sigma_{NC}^{\infty}}\right)^2 - 1} \tag{7}$$

Knowing the characteristic length (a_{ci}), equation (4) gives the fracture strength (σ_{NC}^{∞}) for the specified crack length (2c). Fracture strength (σ_{NC}) of the finite width plate is obtained from equation (5) or dividing (σ_{NC}^{∞}) with the correction factor (Y). It is well known fact that the fracture strength decreases with increase in the crack size. Equation (7) indicates that the characteristic length (a_{ci}) need not be a material constant. This calls for a modification in the inherent flaw model.

A relation between (a_{ci}) and (σ_{NC}^{∞}) in the non-dimensional form is proposed as

$$\frac{\sigma_o \sqrt{\pi a_{ci}}}{K_{IFM}} = 1 - \delta_{aci} \frac{\sigma_{NC}^{\infty}}{\sigma_o} \tag{8}$$

To determine the parameters (K_{IFM} and δ_{aci}) in equation (8), two cracked specimen tests in addition to an unflawed specimen test are required. Normally more tests are performed to take into account the scatter in test results. The parameters K_{IFM} and δ_{aci} in equation (8) are determined by a least square curve fit to the data for a_{ci} and $\frac{\sigma_{NC}^{\infty}}{\sigma_0}$. It should be noted that $\delta_{aci} = 0$ in equation (8) represents the constant damage size. When $\delta_{aci} > 1$ and $\sigma_{NC}^{\infty} = \sigma_0$, equation (8) results $\frac{\sigma_0 \sqrt{\pi a_{ci}}}{K_{IFM}} < 0$. Hence, $0 \leq \delta_{aci} \leq 1$. Whenever δ_{aci} is found to be greater than unity, the parameter δ_{aci} is truncated to 1 by suitably modifying the parameter K_{IFM} with the fracture data. If δ_{aci} is found to be less than zero, the parameter δ_{aci} is truncated to zero and the average of $\sigma_0 \sqrt{\pi a_{ci}}$ values from the fracture data yields the parameter K_{IFM}. Using equations (7) and (8), one can write the following nonlinear equation for the fracture strength (σ_{NC}^{∞}) after eliminating the characteristic length (a_{ci}) as

$$\frac{1}{\pi}\left(\frac{K_{IFM}}{\sigma_{NC}^{\infty}}\right)^2 \left\{1 - \delta_{aci}\left(\frac{\sigma_{NC}}{\sigma_o}\right)\right\}^2 \left\{1 - \left(\frac{\sigma_{NC}}{\sigma_o}\right)^2\right\} = c \tag{9}$$

This non-linear fracture strength equation (9) is solved using the Newton–Raphson iterative scheme to obtain (σ_{NC}^{∞}) for the specified crack size. The fracture strength (σ_{NC}) of the finite width plate is obtained by dividing (σ_{NC}^{∞}) with the correction factor (Y).

A relation between $K_Q \left(\equiv \sigma_{NC}^{\infty} \sqrt{\pi c}\right)$ and $\frac{\sigma_{NC}^{\infty}}{\sigma_o}$ is obtained from equation (9) as

$$\mathrm{K_Q} = \mathrm{K_{IFM}}\left\{1 - \delta_{\mathrm{aci}}\frac{\sigma_{\mathrm{NC}}^{\infty}}{\sigma_0}\right\}\sqrt{1 - \left(\frac{\sigma_{\mathrm{NC}}^{\infty}}{\sigma_0}\right)^2} \qquad (10)$$

Equation (10) represents a failure assessment diagram useful for fracture strength evaluation of different cracked configurations. The fracture strength $\sigma_{\mathrm{NC}}^{\infty}$ versus crack size 2c curves can be generated from equation (9) by specifying $0 < \sigma_{\mathrm{NC}}^{\infty} < \sigma_0$ useful for evaluation of $\sigma_{\mathrm{NC}}^{\infty}$ to any specific crack size. Applying the correction factor *Y* to $\sigma_{\mathrm{NC}}^{\infty}$, the fracture strength (σ_{NC}) can be found.

3. Results and Discussion

Fracture data [13] on high strength alloys useful for aircraft applications is utilized in the present study to verify the validity of the fracture criterion. The unnotched strength (σ_0) data in Table 1 are categorized by material, alloy, temper and / or heat treatment, bare or clad and thickness. Specimen identification is made by lettering LT or TL while generating the plane-stress and transitional fracture toughness data. The first letter indicates the orientation of material of the specimen relative to the direction of stressing and the second, the direction of crack / damage propagation. Average strength value of the multiple test results is considered in the analysis.

A standard error (*SE*) between analytical and test results is obtained from

$$SE = \sqrt{\frac{1}{\mathrm{N}}\sum_{i=1}^{N}\left(1 - \frac{Analysis\,\mathrm{Re}\,sult}{Test\,\mathrm{Re}\,sult}\right)_i^2} \qquad (11)$$

where *N* is the number of test specimens.